Chromatin and Gene Regulatory Dynamics of Optic Nerve Invasion in Retinoblastoma at Single-Cell Resolution

Yihan Zhao [ab1], Peng Liu[a1] , Lei Hu[b1], Mingxi Ke[b], Nan Min[c],

Zehua Zeng [ab*], Hongwu Du [a*]

*Correspondence: zehuazeng@xs.ustb.edu.cn (Z. Zeng),

hongwudu@ustb.edu.cn (H. Du)

[a] Daxing Research Institute, University of Science and Technology Beijing, Beijing 100083, China.

[b] School of Chemistry and Biological Engineering, University of Science and Technology Beijing, Beijing 100083, China

[c] Foreign languages college, University of Science and Technology Beijing, Beijing 100083, China

[1] These authors contributed equally to this work

Address: 112 Lab, Lihua BLDG, No.30 Xueyuan Road, Haidian District, Beijing 100083 China. Prof. Hongwu Du, Email: hongwudu@ustb.edu.cn

Abstract

Retinoblastoma is a rare and aggressive form of eye cancer that arises from the retina's photoreceptor precursor cells. Yet, the mechanism of cancer evolution in optic invasion and the identification of molecularly defined tumor-propagating cells has not been reported. Using single-cell RNA and ATAC sequencing, we uncovered a propagating cell named STER after invasion of the optic nerve. We also report on the dynamic processes of photoreceptor degeneration and optic nerve injury in the retina and identify potential regulatory elements and transcription factors involved. STER cells mediate optic nerve destruction and retinal degeneration during the proliferation and migration of retinoblastoma. Finally, we develop drug sensitivity testing algorithms for malignant clusters, providing potential therapeutic targets and drug predictions for retinoblastoma invasion.

Keywords

Retinoblastoma；Single-cell RNA sequencing；Single-cell ATAC-seq；Bioinformatics

Background

Retinoblastoma is a rare and aggressive childhood cancer, with approximately 8,000 children diagnosed worldwide each year. It is typically caused by biallelic mutations in the retinoblastoma gene (RB1) in a single developing retinal cell.[1][2][3] Most untreated retinoblastomas eventually invade the optic nerve. A study of optic nerve invasion from retinoblastoma reconfirmed that the degree of histopathologic invasion of retinoblastoma into the optic nerve was significantly associated with metastasis.[4]With the development of medical technology, there are many new options for the treatment of retinoblastoma including enucleation, chemotherapy, laser photocoagulation and thermotherapy.[5] [6]Due to the lack of understanding of the pathogenesis of retinoblastoma, enucleation is considered an inevitable step if retinoblastoma lacks early intervention, and accompanied by serious complications

such as edema, conjunctival cyst, pyogenic granuloma, ptosis, blepharoptosis, and superior sulcus defect.[7]

Existing research on retinoblastoma (RB) focuses on transcriptomics and DNA genome research.[8] RB single-cell RNA sequencing (scRNA-seq) enables us to further understand the phenotypic heterogeneity, immune landscape, and metastatic propensity of tumor cells.[9] For example, Wu et al.[9] reveals the landspace of immunosuppressive environment in RB and Yang et al.[10] built an atlas of RB, revealing the origin cells of RB and potential novel switch genes during human RB development. Specifically, a recent study using scRNA-seq and scATAC-seq provides evidence supporting G2/M progenitors as the origin cells of RB.[11] Because the optic nerve is fully developed after birth, single-cell transcriptomics and chromatin-access sequencing in retinoblastoma have distinct discontinuities at different omics layers. This suggests that revealing the dynamics of transcriptional regulation in retinoblastoma helps us find the differentiation point of cancer evolution. In addition, new multi-omics integration algorithms have recently been developed that are anchored from chromatin positions and facilitate the integration of different omics layers for more robust results[12]. These algorithms facilitate the systematic dissection of the multi-omic process of optic nerve invasion. Interest in the mechanisms underlying RB invasion of the optic nerve has been spurred by its metastatic nature. However, existing studies lack effective integration of RB chromatin accessibility and transcript expression, as well as understanding of transcription factor binding heterogeneity and malignant cluster control in RB development.

In our study, we proposed a large scale single-cell multiomics characterization map of retinoblastoma in the course of optic nerve invasion. We selected six single-cell RNA and ATAC samples of optic nerve invasion, and used transcriptional dynamics model and multiomics integration algorithm to reveal the process of optic nerve invasion in the retina. In particular, we identified STER cells, a key intermediate cell involved in tumor metastasis and malignant differentiation, and verified their presence in another large retinoblastoma data set. At the same time, we elaborated the transcriptional regulation dynamics of STER cells and retinal

degeneration and optic nerve invasion, and further revealed the cell differentiation map and carcinogenesis pathology of retinoblastoma. Finally, we evaluated the effectiveness of a series of potential drugs on the inhibition of optic nerve invasion by using tumor cell killing rate and semi-inhibitory concentration IC50 as the criteria for the identification of retinoblastoma drug candidates, providing a new idea for the early intervention of retinoblastoma.

Result

A single-cell regulatory atlas of the optic nerve invasion in retinoblastoma

To capture cellular heterogeneity in retinoblastoma, we used two samples: one with optic nerve invasion (24 months) and one in normal status (4 months), and generated single-cell assay for transposase-accessible chromatin sequencing (scATAC-seq) and single-cell RNA sequencing (scRNA-seq) libraries, respectively (Fig.1A). After quality control and filtering, we obtained 20,037 single-cell transcriptomes and 21,194 single-cell epigenomes. To assess the similarity and diversity between individual cells, we used unsupervised analysis with Uniform Manifold Approximation and Projection (UMAP) for dimensionality reduction and clustering.[13] For both scRNA-seq and scATAC-seq, we used Graph-linked unified embedding (GLUE) to obtain low-dimensional embeddings and cell clustering. Cluster annotations were obtained from differential marker analysis (Fig.1B), and were validated using previously published retinal markers[14] -[17] .

In retinal cells, we have identified photoreceptor cells (high expression of SYT1, PDC, and MAP2) [14], proliferative photoreceptor cells (P-photoreceptor cells) with high expression of CIT and CDCA8**Error! Reference source not found.**, retinal stem cells (high expression of TUBA1A and RBP1)[15] (note: no specific markers were found for this cluster when using various differential expression methods, but

we believe this cluster has stemness and this was confirmed in subsequent temporal analysis), Serotonin and Trefoil factor-expressing Retinal cells (STER) with high expression of TFF1, TPH1, and PHACTR1, Retinal Pigment Epithelial cells (RPE) with high expression of BEST1, RLBP1, and RPE65.[14] Müller glial cells (high expression of VIM, LGALS1, and COL3A1)[16] ,and Astrocytes (high expression of S100A6 and S100A4)[17] (Fig.1C) (Table.S1). Interestingly, in retinoblastoma cells invaded by optic nerve, we almost did not find any photoreceptor cells in any omics level (Fig.1D). This was also not observed in subsequent validations with another dataset, suggesting that it may be a marker for vision loss in patients two years after the disease onset, providing a new direction for our future research.

After merging the datasets, we observed that the low-dimensional representations of RNA and chromatin accessibility were similar, and the changes observed were associated with disease duration (Fig.2A) and cell type transitions. By performing two sequencing experiments on the same sample and analyzing the complementary aspects of gene regulation, including gene expression (scRNA-seq) and gene activity scores based on chromatin accessibility (scATAC-seq), which is defined by the aggregate local chromatin accessibility of genes (hereafter referred to as the "gene activity score"), as well as the aggregate TF motif activity score., we found Corticogenesis TFs such as SOX11 and NHLH2 showed strong cluster-specific enrichments in these three metrics (Fig.1E). SOX11 has been demonstrated to play important roles in various biological processes including neural development, tumor growth, and stem cell fate.[18] [20] It has been found to be overexpressed in multiple cancers, and its expression levels are correlated with cancer cell proliferation and invasion, making it a potential cancer biomarker and therapeutic target. NHLH2's expression is also associated with the occurrence and progression of multiple cancers, such as renal cancer.[21]

Studies have shown that NHLH2 can promote the proliferation and invasion of tumor cells.[22] Interestingly, SOX11 and NHLH2 are highly expressed in STER cells and photoreceptor cells, respectively, but their motifs are almost not accessible in the corresponding cells. We believe that this may be due to chromatin inaccessibility

resulting from the differentiation endpoint. In addition, the correlation between the eight cell types was similar in terms of RNA expression and chromatin activity, with photoreceptor cells and STER cells being the most similar. However, in the motif scores, it clearly distinguished the two stages of motif enrichment (Fig.1F).

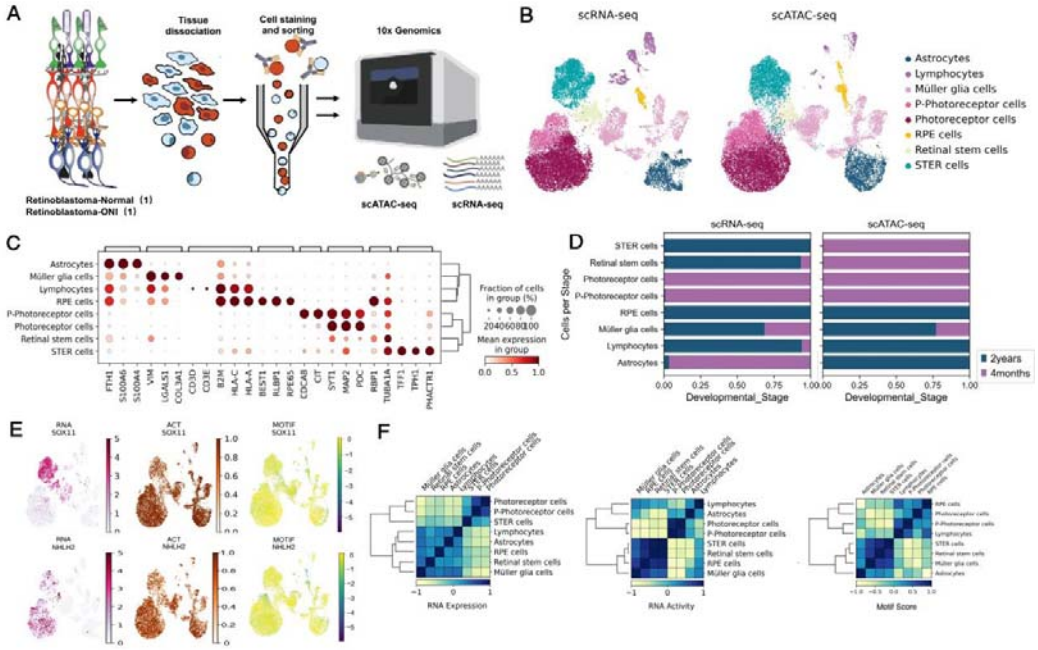

Figure 1 A single-cell epigenomic atlas of the optic nerve invasion retinoblastoma.

(A) Schematic of samples, profiling methods, and cell types.

(B) UMAP of cells colored by cluster. P-Photoreceptor cells, Proliferation-Photoreceptor cells; RPE cells, Retinal pigment epithelial cells; STER cells, Serotonin- and Trefoil factor-expressing Retinal cells.

(C) Dotplot showing the cells expression selected markers across scRNA-seq clusters.

(D) Fraction of each cell type isolated from development stage from 4months and 2 years samples.

(E) Multiomdal profiling of SOX11, and NHLH2 including gene expression (scRNA-seq), gene activity scores, and TF motif activity (scATAC-seq).

(F) The correlation matrix between different celltype from multi-omics.

Epigenetic regulators of a novel retinoblastoma cell STER

We have identified and characterized a novel cell type, Serotonin and Trefoil factor-expressing Retinal cells, which are characterized by the expression of serotonin and trefoil factor genes, as well as high levels of the transcription factor SOX11. We hypothesize that these cells are unique to retinoblastoma invading the optic nerve and

may play a critical role in controlling the process of optic nerve invasion. In the previous study, we obtained the relationship between gene and chromatin regulation, and these regulatory genes may be related to STER cells. Therefore, we conducted a series of analyses based on this new cell type. We calculated the cosine similarity of the GLUE features of RNA-gene and ATAC-peak, and found the peak with the highest correlation, and considered the gene and peak as a cis-regulatory element. For the analysis of the regulatory genes in STER cells, we extracted such cis-regulatory elements (Fig.2B) and intersected them with the top 50 differentially expressed genes in each cell, resulting in five STER-specific regulatory genes: TFF1, TUBB2B, SSTR2, GMNN, and SOX4. (Table.S4, 5) (Fig.S3)

These five genes are closely related to tumor formation and metastasis, and we selected two more functionally relevant representative marker genes of STER cells, SOX4 and TUBB2B for further study. SOX4 is a gene that encodes a transcription factor, and its expression level is significantly increased in various cancers. SOX4 plays a role in promoting cancer cell proliferation, invasion, and metastasis during cancer development, and its overexpression can promote the growth, invasion, and metastasis of retinoblastoma cells, which is closely related to the malignancy of tumors.[24] [25] Studies have also shown that loss of the SOX4 gene can make tumor cells sensitive to chemotherapy and reduce their ability to metastasize.[26] TUBB2B is a gene that encodes a microtubule protein, and its function involves microtubule dynamics, cell morphology maintenance, cell division, and neuron development. Research has found that TUBB2B has drug resistance in retinoblastoma treatment, indicating that cells with high TUBB2B expression are more difficult to kill with therapeutic drugs, thus promoting tumor metastasis.[27] [28] Both of these genes are associated with tumor metastasis and cancer cell proliferation, and their high expression in STER cells further validates the malignancy of these cells and their importance in the differentiation process of retinoblastoma.

Based on the characteristic enhancer activity of TUBB2B and SOX4 in both photoreceptor cells and STER cells (Fig.2C), we inferred that both genes are involved in retinal neural signaling. SOX4 motifs are enriched in retinal ganglion cells and

photoreceptor cells, while TUBB2B motifs are enriched in retinal ganglion cells (Fig.2D-E). Although chromatin accessibility is low in both STER and photoreceptor cells, SOX4 and TUBB2B are highly expressed in both cell types. Furthermore, we performed functional enrichment analysis on the top 100 marker genes in STER cells, which showed that GO biological processes are mainly associated with neuronal development and DNA replication, while GO molecular functions are mainly related to DNA transcription binding (Fig.2F). This may be a manifestation of cell proliferation and differentiation towards cancer cells after gene mutations in retinal cells. Additionally, pathway enrichment analysis revealed that STER cell-related genes are enriched in the retinoblastoma pathway, indicating that this cell type has considerable specificity for retinoblastoma (Fig.2G).

To validate the existence of STER cells, we selected another publicly available retinoblastoma dataset (GSE168434) as a validation dataset for result verification. In this dataset, we annotated 91,489 cells with their corresponding marker genes into six cell subtypes, including retinal neurons, cone precursor cells, microglia cells, retinoblastoma cells, rod cells, and STER cells (Fig.S1A-D). In the validation dataset, we found that the proportion of STER cells increased in the subtypes of retinoblastoma invasion (Fig.S1E) and appeared as the endpoint of the differentiation trajectory (Fig.S1F), which is highly consistent with our analysis in the analyzed dataset.

We observed that the upregulated TFF1 gene in the analyzed dataset was also highly expressed in the validation dataset in the invasive cells (Fig.S2A;D-E). We were particularly interested in the performance of STER cells in the validation dataset, so we extracted STER cells (Fig.S2B-C) and found that the Hypoxia pathway was significantly upregulated in the invasive STER cells, indicating a metabolic reprogramming process, which is also an important hallmark of cancer development[29] [30] (Fig.S2F). We also found this in the pathway enrichment of upregulated genes relative to cone cells and in the pathway enrichment of invasive cells relative to non-invasive cells in the entire dataset (Fig.S2G-H). During the pathway enrichment process, we also discovered the upregulation of glycolysis in the invasive STER cells,

indicating a new metabolic pathway in cancer cells (Fig.S2I).

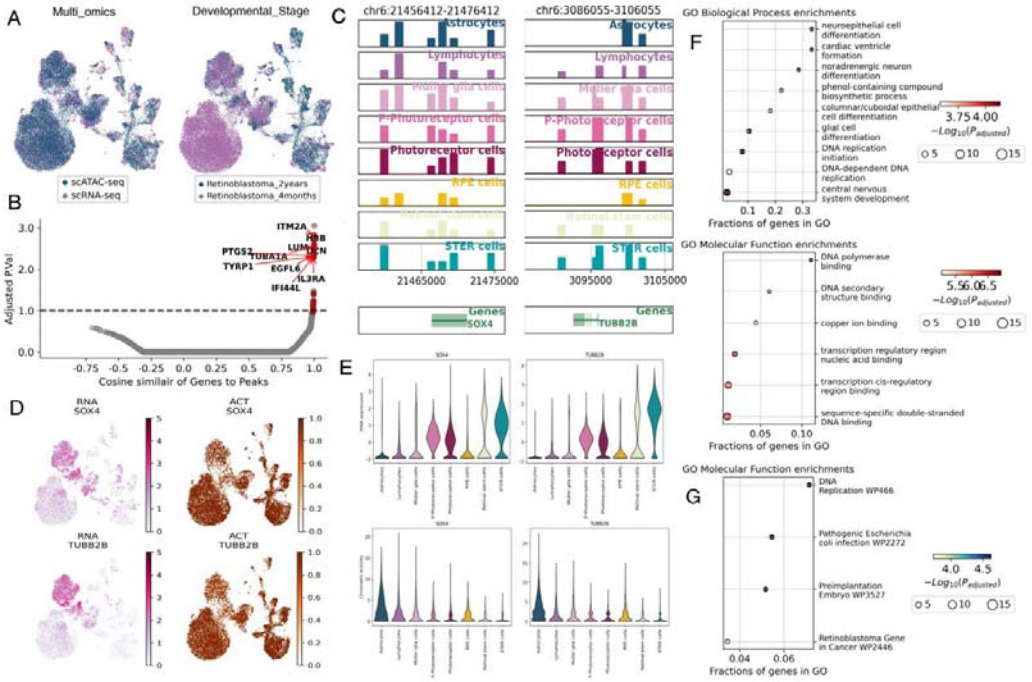

Figure 2 Epigenetic regulators of a novel retinoblastoma cell STER.

(A) UMAPs of scRNA-seq and scATAC-seq intergrated and colored by omics and developmental stages.

(B) Correlation plot of gene expression and activity in a cell

(C) Genomic tracks for accessibility around SOX4 and TUBB2B for different retinoblastoma cell types. Peaks called in the scATAC-seq data.

(D) UMAPs of the RNA expression value and Chromatin activity for SOX4 and TUBB2B. The RNA expression plotted is the expression in the nearest RNA cell following integration of the scRNA-seq and scATAC-

(E) Corresponding violin plots and boxplots quantifying integrated SOX4 and TUBB2B expression and activity for cells in each cell type. the right. Boxplots represent the median, 25th percentile and 75th percentile of the data, and whiskers represent the highest and lowest values within 1.5 times the interquartile rang

(F) GO Biological and Molecular enrichment analysis of top 100 marker genes of STER cells.

(G) Wiki pathway enrichment analysis of top 100 marker genes of STER cells

Transcriptional dynamics of retinal cells in retinal degeneration.

In this study, we analyzed the transcriptional dynamics of retinal cells to identify transcriptional changes associated with retinal degeneration after optic nerve invasion.

We extracted a total of 13,315 functional retinal cells, including photoreceptor cells, retinal stem cells, and STER cells(Fig.3A). Using the ratio of spliced to unspliced transcripts, we calculated RNA velocity for these cells [31] and examined the transcriptional dynamics of retinal functional cells. We used PyVIA to calculate the pseudotime values for each cell based on RNA velocity and found that retinal stem cells had the lowest pseudotime value, while p-photoreceptor cells and STER cells were the endpoints of two differentiation trajectories (Fig.3C-E).

Then, we recalculated the neighborhood maps of each cell and re-annotated the subtypes of retinal ganglion cells. We obtained cluster annotations from differential marker analysis (Fig.3B) and confirmed them using previously described markers and their known functions in the literature. Based on high expression of STXBP5L, MYO3A, and GRM8, we identified cone photoreceptor cells,[14] where both STXBP5L and GRM8 are involved in the release of neurotransmitters[32] ; based on expression of CENPF, GTSE1, and APOLD1, we identified proliferative-photoreceptor cells (P-photoreceptors), where CENPF and GTSE1 are involved in cell proliferation processes[33] ; based on expression of CAMK1D and PDC, we identified rod photoreceptor cells[14] ; based on expression of ZFAS1 and USPL1, we identified T-cell receptor photoreceptor cells (TCR-photoreceptors), which help protect the retina from light damage and infection by recognizing light-responsive proteins[34] ; and based on expression of PHACTR1 and BASP1, we identified STER cells (Fig.3G) (Table.S2).

To identify the genes most likely to be involved in retinal ganglion cell differentiation, we calculated the latent time of the dynamic model of retinal cells and identified the driving genes with high probability in the dynamic model. We extracted the highest probability genes per week based on a threshold of 0.2 and identified 44 genes that influence differentiation transcription dynamics (Fig.3F). We found that TAFA4 and CAMK1D were the most correlated genes with transcriptional models in TCR and cone cells, and they had similar differentiation endpoints (Fig.3H), with both genes having positive RNA velocity rates (Fig.3I). Research has shown that TAFA4 and CAMK1D play a role in protecting neurons and promoting the

development and survival of nerve cells in the nervous system. The pseudotime analysis results demonstrated that TCR and cone cells are intermediate cells differentiated from stem cells, which may indicate that TAFA4 and CAMK1D are key gene targets for the treatment of retinal deformation.

According to the dynamic heatmap of gene expression over time, we can see that for P-photoreceptor cells, the highly correlated genes are APOLD1 and GTSE1, which have similar characteristics in cell proliferation and invasion. The reason for changes in RNA velocity may be that P-photoreceptor cells appear first in patients with retinal degeneration, followed by the loss of photoreceptor cells, leading to a decrease in gene expression. For intermediate/rod photoreceptor cells, the related genes are PCLO and PPP2R2B, which are associated with the basic functions of cells. For STER/retinal stem cells, the related genes are BASP1 and OTX2, where the protein encoded by BASP1 is a neuron-specific protein involved in the differentiation process of neurons and may be closely related to retinal degeneration.

To further investigate the causes of retinal degeneration, we performed transcriptome and chromatin activity differential expression analysis on retinoblastoma cells that had undergone retinal degeneration compared to normal retinoblastoma cells. We identified 853 differentially expressed genes, among which SYT1 and PDC were found to be jointly downregulated at the transcriptional and chromatin activity levels in samples taken over two years, commonly seen in multiple types of photosensitive cells (Fig.3J-K). SYT1 has a neuroprotective function, and both genes are involved in the basic functional processes of retinal cells[35]

Finally, we conducted functional enrichment analysis on different subtypes of retinal functional cells and found that cone photoreceptor cells were enriched in glycolysis processes, P ganglion cells were enriched in mitotic cells and cell cycle processes, and rod photoreceptor cells were enriched in ATP synthesis. These processes were downregulated after invasion of the optic nerve (Fig.3L), which may be related to the previous gene downregulation.

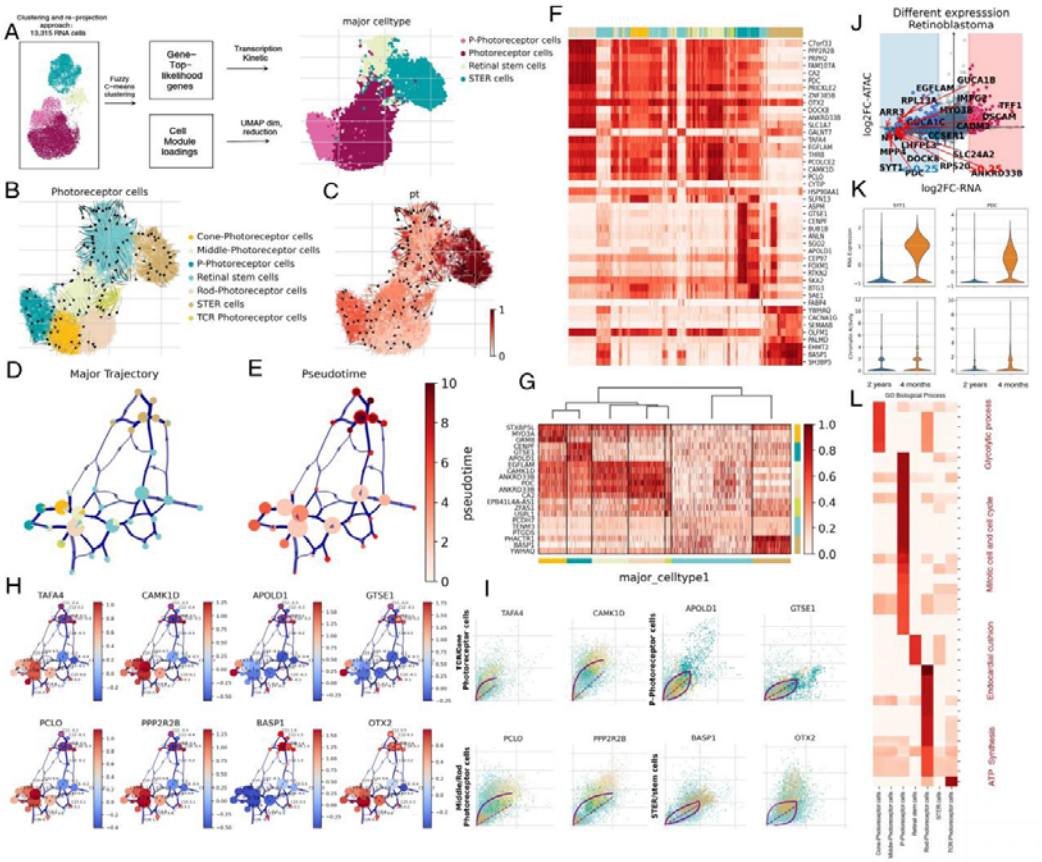

Figure 3: Transcriptional Dynamics and Regulatory Logic of Retinal Degeneration.

(A)Diagram illustrating the clustering and re-projection of expression profiles of functional retinal cells. The dots on the right panel correspond to a UMAP with reduced dimensions.

(B)UMAP plot of scRNA-seq retinal cells isolated from retinoblastoma, with cells colored by subtypes.

(C)Feature plot displaying the pseudo-temporal ordering of retinal cells.

(D)VIA plot colored by cell type proportions in different state nodes.

(E)VIA plot colored by inferred pseudo-temporal ordering. Identified terminal state nodes are outlined in red and labeled according to their representative annotated subtypes.

(F)Heatmap showing expression changes of dynamic genes under the retinal cell dynamic velocity model (with highest probability >0.2).

(G)Heatmap showing expression of selected genes in retinal cell subtypes.

(H)VIA plot showing likely genes by cell subtype in the pseudo-temporal trajectory.

(I)RNA velocity dynamics test for top 2 likely genes in each cell subtype (purple lines represent the dynamic trend of all immune cells, black lines represent the dynamic trend of subtypes, horizontal axis represents splicing, vertical axis represents unspliced mRNA abundance).

(J)Differential gene expression and gene activity analysis between retinoblastoma in the period of optic nerve invasion and normal staging (point size represents the log10 p-value of genes).

(K)Corresponding violin and box plots used to quantify integrated SYT1 and PDC expression and activity in cells within 4 months and 2 years.

(L)GO biological process enrichment analysis of the top 50 marker genes for each cell subtype using

t-tests.

Transcriptional Dynamics of Retinal Ganglion Cells in Optic Nerve Damage.

We have analyzed the transcription dynamics of retinal ganglion cells to study transcriptional changes associated with neuronal optic nerve damage. We extracted 6,677 retinal ganglion cells from all cells, including astrocytes, lymphocytes, Muller glial cells (MGC), and RPE cells (Fig.4A, Fig.S4A).

We calculated the RNA velocity of these cells based on the proportion of spliced/unspliced transcripts and detected the transcription dynamics of retinal functional cells. Using PyVIA, we calculated the pseudotime states of each cell based on RNA velocity and found that astrocytes with high expression of CLU were a significant differentiation endpoint (Fig.4B-C, Fig.S4C).

Next, we recalculated the neighborhood graph of each cell and re-annotated the subtypes of retinal ganglion cells (Fig.S4B). Cluster annotations were derived from differential marker analysis (Fig.S4D) and confirmed using previously described markers and their functions in the literature. Within the retinal ganglion cells, we identified CLU-positive astrocytes as a distinctive population with high expression of CLU and PERP. Furthermore, CLU-positive astrocytes also exhibited high expression of KRT19, a marker frequently used as a tumor biomarker in therapy, and found to be highly expressed in various types of tumors[36] .

We identified MGC immune cells using lymphocyte markers and high expression of VIM and ADGRL4[37] . MGC normal cells were identified based on high expression of THBS2 and LGALS1. MGC-profiled cells were identified based on the expression of FHL1 and CIS genes. Small glial cells were identified based on the expression of PEBP1, CDH19, and lymphocyte markers[38] . Astrocytes with high expression of PHACTR1 were identified as a distinctive population based on this marker. Fibrous astrocytes were identified based on the expression of PDC and CA2[39] , and peduncular astrocytes were identified based on LINC02444. T cells

were identified based on the expression of CD3D and CD3E (Fig.4D) (Table.S3).

To identify genes involved in the differentiation of retinal ganglion cells, we calculated the latent time of the dynamic model and identified driver genes in the model. We extracted the top driver gene for each subtype based on a threshold of 0.25 and identified 55 genes that affect transcriptional dynamics of differentiation (Fig.4E). Among these genes, FOSB, which is highly expressed in small glial cells, and CLDN4, which is highly expressed in CLU+ astrocytes, have been shown to promote proliferation of tumor cells. This suggests that upregulation of these two genes may be key to retinal ganglion cell damage.

We also investigated the role of STER cells in the invasion of the optic nerve. Using CellphoneDB[40], we calculated the interactions between STER cells and optic nerve cells and found that STER cells mainly affect MGC-profiled cells through the receptor EFNB2 and EPHB2 (Fig.4F-G). These proteins belong to the Eph/ephrin family of cell surface receptors and ligands, which play critical roles in mediating cell-to-cell communication and regulating various cellular processes such as adhesion, migration, differentiation, and survival[41] [44].

In addition, we also studied the transcriptional dynamics of the MGC-profiled genes PDGFD, SERPING1, FAM11BA, and FOSB. Among these genes, FAM11BA showed a relatively more significant upregulation, indicating its greater activity in the invasion process of the optic nerve. Abnormal expression of FAM11BA has been reported to be associated with the occurrence of various diseases and may also be involved in the pathogenesis of neurodevelopmental and neurodegenerative diseases.

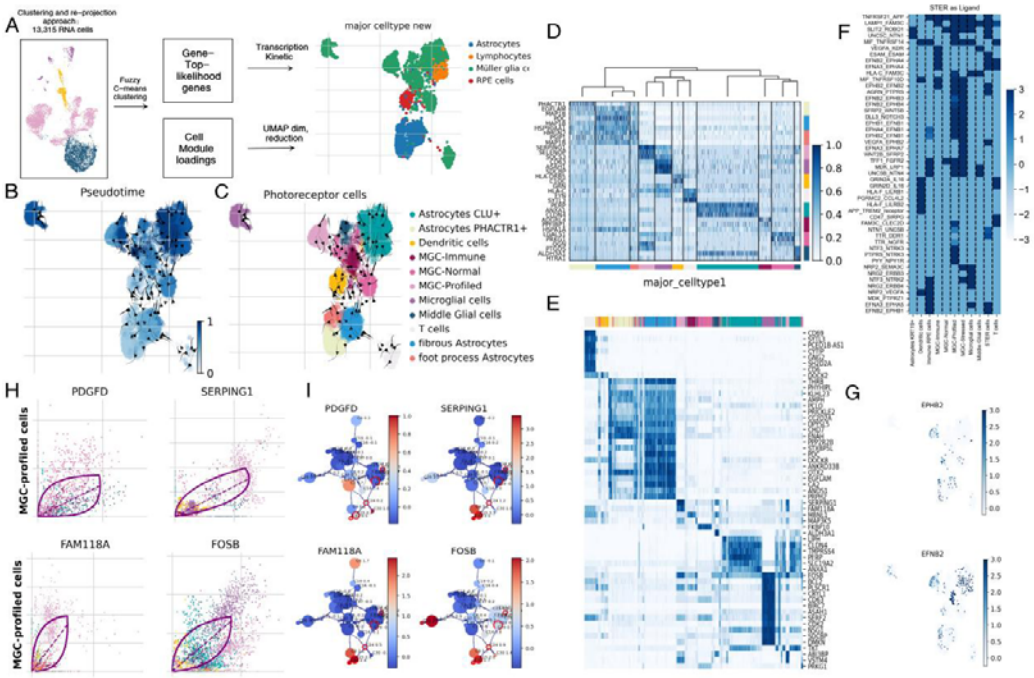

Figure 4: Transcriptional dynamics and cell-cell interactions in optic nerve damage.

(A) Illustration of clustering and re-projection of retinal ganglion cells based on expression. Points in the panel on the right correspond to the new dimension reduction UMAP.

(B)Feature plot displaying pseudotemporal ordering of retinal ganglion cells.

(C)UMAP projection of scRNA-seq retinal ganglion cells isolated from retinoblastoma, color-coded by subtype.

(D)Heatmap displaying expression of selected genes in retinal ganglion cell subtypes.

(E)Heatmap showing expression changes of dynamic genes in retinal ganglion cells under a dynamic velocity model (highest probability > 0.2).

(F)Cell-cell interactions between STER cells and retinal ganglion cells through CellphoneDB.

(G)UMAP displaying expression of EFNB2/EPHB2 as STER cell receptors in retinal ganglion cells.

(H)VIA plot displaying top 2 probable genes of cell subtypes in the pseudotemporal trajectory (left). RNA velocity dynamics test of top 2 probable genes of cell subtypes (right).

Prediction of specific drug candidates for retinoblastoma based on scRNA-seq analyses.

Limited methods currently exist on the treatment of retinoblastoma, and they mostly involve different types of radiotherapy and chemotherapy, which lack clinical specificity[45] . To identify potential drug responses to retinoblastoma, we distinguished normal cells and tumor cells using scRNA-seq. The inference of copy number variations (CNVs) was performed with the python package inferCNV, and the

lymphocytes were used as reference cells with no prominent CNVs (Fig.5A-B; 5E). The acquisition and loss of chromosomes based on single cell transcriptomics to infer CNVs has been widely used in scRNA-seq research, to identify whether cells are malignant tumor cells[46] . The cells with highly CNVs score were marked as tumor cells, and 3097 STER cells were identified as tumor cells (Fig.5D).Louvain algorithm was used to cluster tumor cells and 4 clusters of them were identified with different distribution (Fig.5E).

To identify the specific drugs of retinoblastoma, scDrug was used to predict the potential drug responses based on the transcriptomic of tumor cells. Gene expression profiling data of CCLE cell lines and GDSC dataset were used as training data, including data on 1379 tumor cell lines and 1018 tumor cell lines respectively, and drug-cell lines response data of GDSC dataset and PRISM repurposing dataset were used as training and testing labels. The half maximal inhibitory concentration (IC50) and tumor cell killing ratio predicted by scDrug was used as selection criteria to identify candidate drugs for retinoblastoma. Based on these criteria, Two most effective potential drugs were identified for retinoblastoma: GSK1070916, a highly effective Aurora B/C kinase inhibitor with extensive anti-tumor activity in tissue cultured cells and human tumor xenotransplantation models, exhibiting the highest tumor cell killing ability in the prediction of scDrug[47] , and Epothilone B, a kind of non taxus antitubulin polymerized anti-tumor drug that shows the lowest IC50 in the prediction of scDrug, and has recently been proposed for cancer treatment, especially in breast cancer[48] (Fig.5F-G).

The cell killing percentage of different drugs showed no significant correlation with 1-IC50, possibly due to different calculation principles. By studying the intersection of two indicators, it was found that lspinesib Mesylate, a drug that induces cell cycle arrest, has high cell killing percentage and low IC50, and has the potential to treat retinoblastoma[49] (Fig.5H-I).

To determine the treatment mechanism of Lspinesib Mesylate, we conducted gene sets enrichment analysis using the Gene Ontology database. Our analysis revealed highly enriched gene sets in tumor cells (STER cells) such as cell cycle, attachment of mitotic spindle microtubules to kinetochore, and DNA damage response (Fig.5J). We would like to emphasize that the enrichment of cell cycle and microtubule activity might be the reason why retinoblastoma may be sensitive to Lspinesib Mesylate.

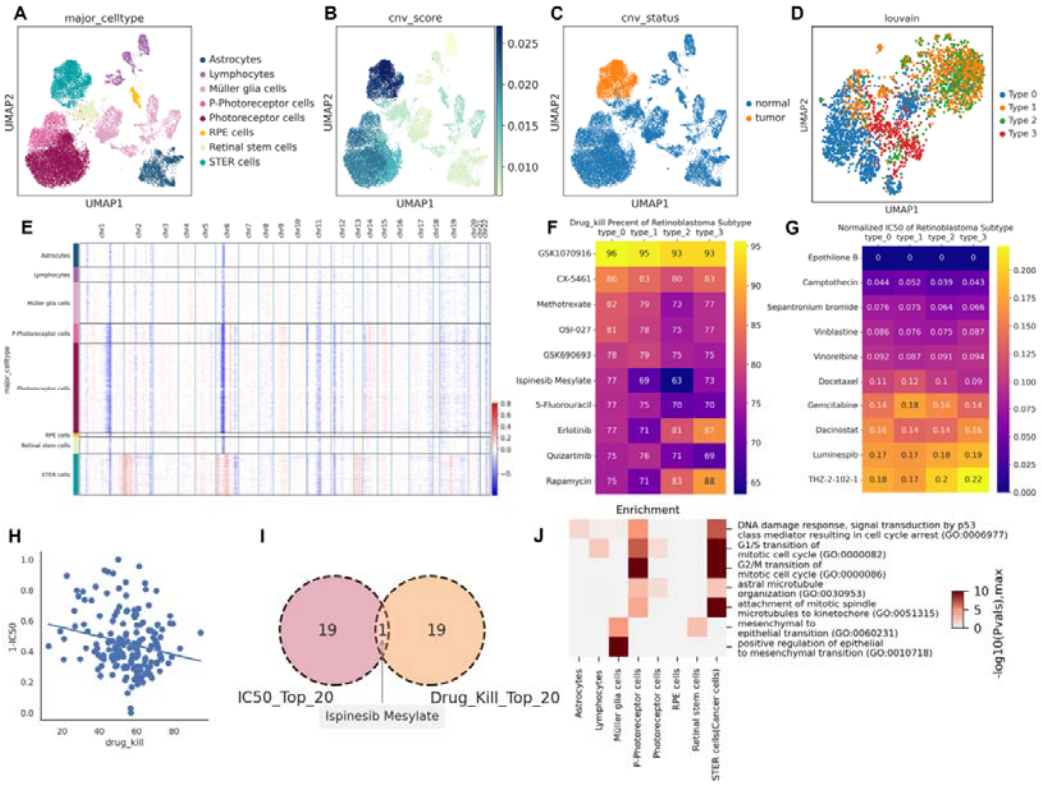

Figure 5: Prediction of specific drug candidates for retinoblastoma based on scRNA-seq analyses.

(A-C) Umap plot of cells by clusters based on scRNA-seq, color-coded by cell types, CNVs scores and tumor types.

(D) Umap plot of tumor cells by louvain clusters, color-coded by the louvain clustering types.

(E) The upper panel exhibiting large-scale CNVs of single cells inferred based on lymphocytes.

(F) Heatmap displaying the drug killing percent of retinoblastoma clusters, color-coded by the drug killing percent.

(G) Heatmap displaying the normalized IC50 of retinoblastoma clusters, color-coded by the normalized IC50.

(H) The scatter plot depicting the correlation between 1-IC50 and drug killing percent.

(I) The venn plot revealing the intersection between the 20 drugs with smalest IC50 and the 20 drugs with the highest percentage of killing.

(J) Heatmap displaying the enrichment pathways of different clusters, color-coded by the

-log10(P-values).

Discussion

We used single-cell transcriptomics and chromatin accessibility sequencing to characterize the phenotypic heterogeneity, transcriptional regulatory relationships, and multicellular ecosystems of RB. Overall, our study describes the transcriptional dynamics of retinal cell degeneration and optic nerve invasion in RB, establishes a comprehensive tumor immune microenvironment (TME) map of RB, including the malignant cluster STER and the phenotypic classification of optic nerve and photoreceptor cells, as well as intercellular communication within the TME.

STER cells are a unique malignant cluster that is exclusively associated with optic nerve invasion, and their origin cells can be traced back to the photoreceptor precursor cells. We also found this type of cell in the public database of RB. The characteristic genes of STER cells are mainly the nuclear transcription factor SOX4, which is commonly associated with epithelial-mesenchymal transition (EMT)[49] , and the microtubule protein TUBB2B, which is a marker of the optic nerve[51] . Functional enrichment analysis of STER cells revealed a strong association with retinoblastoma, DNA replication, and nervous system development. We detected very few STER cells in non-invasive retinoblastoma, indicating that STER cells are specific to optic nerve invasion.

Inhibition of retinal degeneration provides a new prospect for RB treatment, especially for patients who want to preserve their eyes. We calculated the transcriptional dynamics of photoreceptor cells transforming into malignant clusters in the retina, constructed a dynamic model of malignant clusters and normal photoreceptor cells, and identified the gene mucin-associated adhesion molecule BASP1, which is involved in the evolution of malignant clusters. The activation of BASP1 is of great significance for the invasion of retinoblastoma. The study of the interaction between malignant clusters and optic nerve cells provides us with an

effective strategy for designing inhibitors of malignant cluster activity. We have developed a framework that can predict potential drug treatment regimens based on the drug sensitivity of different cells and their IC50 values. In the future, we envision achieving the therapeutic effect of retinoblastoma by deactivating malignant clusters.

However, our study has several limitations. Firstly, we only used two samples to explore the mechanism of optic nerve invasion. Although we validated the existence of the malignant cluster STER in public databases, RB exhibits intratumoral heterogeneity. Thus, we need to verify the presence of STER in more individuals with optic nerve invasion and compare them with normal retinal cells in biopsy samples. Secondly, in many cases, mRNA is not an exact indicator of protein expression. Therefore, the expression of the receptor proteins predicting the interaction between STER and optic nerve is not entirely correlated. However, as this area has not been studied extensively, we can validate our findings through western blotting in future research and attempt to use drugs to inhibit the interaction between STER and other cells.

Overall, our research provides a comprehensive analysis of single-cell epigenomics and transcriptomics, as well as transcriptional dynamics, for the interaction between retinoblastoma cells and photoreceptor cells in retinoblastoma. Our findings demonstrate the unique power of single-cell epigenomics in predicting chromatin regulation during tumor metastasis, providing new targets and evidence for the development of retinoblastoma therapies in the future.

Methods

Data extraction

The raw expression matrices of scRNA-seq and scATAC-seq of the retinoblastoma were

retrieved from National Center for Biotechnology Information Gene Expression Omnibus under accession number GSE166173 and GSE166174.

Data validation

The original expression substrate of retinoblastoma SCRNA-seg was retrieved from the National Center for Biotechnology Information Gene Expression Integration, accession number GSE168434.

scRNA-seq preprocessing[52]

Raw sequencing data were converted to fastq format using the command 'cellranger mkfastq' (10x Genomics, v3.1.0). scRNA-seq reads were aligned to the GRCh38 (hg38) reference genome and quantified using 'cellranger count' (10x Genomics, v.3.1.0). 'Velocyto' (v.0.17.17)(La Manno et al., 2018)was used to obtain splicing-specific count data for downstream RNA velocity analysis. Count data was further processed using the 'Scanpy' Python package[53] (v.1.8.2)(Wolf et al., 2018). We removed cells with less than 200 informative genes expressed, cells with more than 4300 genes expressed and cells with more than 25% of counts corresponding to mitochondrial genes. We removed genes with less than 3 cells expressed. We performed doublet analysis using the 'Scrublet' Python package from scanpy[54] (Wolock et al., 2019), and apply doublet filtering to remove doublets biasing. Count data was log-normalized and scaled to 10,000. We performed high variable gene analysis based parameter setting: 'min_mean=0.0125', 'max_mean=3', 'min_disp=0.5'. Then using PCA embedding to calculate a UMAP layout(Becht et al., 2019). Clusters were identified using the Leiden algorithms(Traag et al., 2019) based on the nearest neighbor graph.

scATAC-seq preprocessing

Raw sequencing data were converted to fastq format using 'cellranger-atac mkfastq' (10x Genomics, v.1.2.0). scATAC-seq reads were aligned to the GRCh38 (hg38) reference genome and quantified using 'cellranger-atac count' (10x G

enomics, v.1.2.0). Fragment data was further processed using the 'ChrAccR' R package (v.dev.0.9.11+). We filtered out cells with less than 1,000 or more than 50,000 sequencing fragments. TSS enrichment was computed as a metric of signal-to-noise ratio using methods described in (Granja et al., 2019) and we discarded cells with a TSS enrichment less than 4. Fragments on sex chromosomes and mitochondrial DNA were excluded from downstream analysis.

Data preprocessing for cell paired

To preprocess the scRNA-seq for cell paired, we annotated cell types from scRNA-seq data. To preprocess the scATAC-seq for cell paired, we apply the latent semantic indexing (LSI) for dimension reduction and first encoder transformation. Then we constructed the prior regulatory graph to utilized the multi-omics alignment by GLUE[Error! Reference source not found.] (version 0.3.2)(Cao et al., 2022).

Pairing the scRNA-seq and scATAC-seq data by scglue

After constructed the prior regulatory graph from scRNA-seq and scATAC-seq, we specify the probabilistic generative model negative binomial distribution (NB) for the omics-layer to be integrated. Next, we initialize a GLUE model for scRNA-seq and scATAC-seq layers. With the trained GLUE model, eigenvectors for each cell (feature embeddings) were obtained by parameter 'X_glue'. Subsequently, Pearson coefficients were used to find the two most similar feature vectors in scRNA-seq and scATAC-seq. Duplicate paired cells are discarded in this process.The cell annotations of scRNA-seq were transferred to the corresponding scATAC-seq cells.

Definition of RNA velocity and latent time in sub-celltype trajectories

We computed RNA velocity from Spliced and unspliced read counts generated from FASTQ files using velocyto and scVelo(v.0.2.4) toolkit. We filtered the sub-dataset using the scVelo function 'pp.filter_genes' (min_shared_counts=20).

We then used ‘tl.recover_dynamics’ to revover dynamical model and learn the full transcriptional dunamics of splicing kinetics, ‘tl.velocity’ with mode = ‘dynamical’to compute cell velocities and ‘tt.velocity_graph’ to compute a velocity graph. To compute cell latent time, we used ‘tt.terminal_states’ and ‘tl.latent_time’. This latent time represents the cell’s internal clock and approximates the real time experienced by cells as they differentiate, based only on its transcriptional dynamics. We also computed PAGA velocity graph for trajectory inference from ‘tl.paga’. and detected cell cycle by RNA velocity, which is biologically affirmed by cell cycle scores (standardized scores of mean expression levels of phase marker genes).

Putative interactions between cell types

To enable a systematic analysis of cell-cell communication, we used CellPhoneDB(Efremova et al., 2020). CellPhoneDB is a manual curated repository of ligands, receptors and their interactions, integrated with a statistical framework for inferring cell-cell communication networks from single cell transcriptome data. Briefly, in order to identify the most relevant interactions between cell types, we looked for the cell-type specific interactions between ligands and receptors. Only receptors and ligands expressed in more than 10% of the cells in the specific cluster were considered. We performed pairwise comparisons between all cell types. First, we randomly permuted the cluster labels of all cells 1000 times and determined the mean of the average receptor expression level of a cluster and the average ligand expression level of the interacting cluster. For each receptor-ligand pair in each pairwise comparison between two cell types, this generated a null distribution. By calculating the proportion of the means which are as or higher than the actual mean, we obtained a p-value for the likelihood of cell type-specificity of a given receptor-ligand complex. We then prioritized interactions that are highly enriched between cell types based on the number of significant pairs and manually selected biologically relevant ones. For the multi-subunit heteromeric complexes, we required that all subunits of the co

mplex are expressed (using a threshold of 10%), and therefore we used the me mber of the complex with the minimum average expression to perform the ran dom shuffling.

Gene Ontology (GO) and Network-based Analyses of cell subpopul ations

We performed gene set enrichment analysis of GO terms using gseapy (v.0. 10.8)[55] (Fang et al., 2022) with default parameters (adjusted p-values <0.05) a nd select geneset 'GO_Biological_Process_2021' and 'GO_Molecular_Function_2 021'[56] (Xie et al., 2021). We also calculated the fraction of each GO term usi ng 'Overlap' based on the results of the enrichment analysis, and logarithmized the adjusted P-value. To distinguish the different Go terms, we transformed th e gene of each term into a one-hot code and clustered the terms using 'cluster map' of Python package seaborn (v.0.11.2)[57] (Waskom, 2021) to find similar te rm modules. For network-based analyses, protein lists were submitted to the S TRING-db tool[58] (Szklarczyk et al., 2021) (all active interaction sources, intera ction score > 0.8). The network was exported into a simple tabular output, ref ormatted to display desired parameters (e.g., K-means clusters)

Calculation of motif score

We used scbasset (v.0.0.0)[59] (Yuan et al., 2022)to score motifs on a per c ell basis using motif injection method. For motif injection, we first generated d inucleotides shuffled background sequences, and inserted motif of interest to th e center of those sequences.

Drug response prediction

We mainly used scDrug[60] , a Python package based on the CaDRReS mo del, to predict IC50 values and tumor cell killing ratios of potential drug respo nses. The tumor cells obtained by inferCNV inference were used as input data

for scDrug. We used the seaborn package (version 0.12.2) to visualize the magnitude of IC50 values and tumor cell killing ratios for different subpopulations and to select drugs based on IC50 minimum and tumor cell killing ratio maximum.

Declarations

Ethics approval and consent to participate

Not applicable.

Consent for publication

Not applicable.

Availability of data and materials

Raw sequencing data have been deposited into the National Center for Biotechnology Information Gene Expression Omnibus under accession number GSE166173, GSE166174 and GSE168434. And the preprocessing data and origin code used for this paper will be available after manuscript accept.

Competing interests

The authors declare that they have no competing interests.

Authors' contributions

Y.Z, P.L., L.H. conceived and designed the study. Z.Z.updated the algorithm and completed data integration. Y.Z. analyzed and explained the transcriptional kinetics of retinoblastoma. P.L. conducted validation of the newly discovered cell STER on other datasets. L.H. performed retinoblastoma-specific drug candidate prediction and validation. M.K. and N.M. contributed to the refinement of the analysis process and the addition of the charts. Z.Z. and H.D. supervised the project and contributed to the conception of the project. Y.Z, P.L. and L.H. wrote the manuscript with contributions from the co-authors. All authors read and approved the final manuscript.

Acknowledgements

This work was financially supported by the Fundamental Research Funds for the Central Universities (FRF-TP-22-007A1), the Hebei Provincial Department of Science and Technology (No.19942410G), and the Student Research Training Program of University of Science and Technology Beijing.

Reference

[1] Comings D E. A general theory of carcinogenesis[J]. Proceedings of the National Academy of Sciences, 1973, 70(12): 3324-3328.

[2] Friend S H, Bernards R, Rogelj S, et al. A human DNA segment with properties of the gene that predisposes to retinoblastoma and osteosarcoma[J]. Nature, 1986, 323(6089): 643-646.

[3] Knudson Jr A G. Mutation and cancer: statistical study of retinoblastoma[J]. Proceedings of the National Academy of Sciences, 1971, 68(4): 820-823.

[4] Magramm I, Abramson DH, Ellsworth RM. Optic nerve involvement in retinoblastoma. Ophthalmology 1989; 96:217-22.

[5] Ancona-Lezama D, Dalvin LA, Shields CL. Modern treatment of retinoblastoma: A 2020 review. Indian J Ophthalmol. 2020 Nov;68(11):2356-2365. doi: 10.4103/ijo.IJO_721_20. PMID: 33120616; PMCID: PMC7774148.

[6] De Potter P. Current treatment of retinoblastoma[J]. Current opinion in ophthalmology, 2002, 13(5): 331-336.

[7] Chintagumpala M, Chevez-Barrios P, Paysse E A, et al. Retinoblastoma: review of current management[J]. The oncologist, 2007, 12(10): 1237-1246.

[8] Xu, X., Singh, H., Wang, L. et al. Rb suppresses human cone-precursor-derived retinoblastoma tumours. Nature 514, 385–388 (2014). https://doi.org/10.1038/nature13813

[9] Knudsen ES, Wang JY. Targeting the RB-pathway in cancer therapy. Clin Cancer Res. 2010 Feb 15;16(4):1094-9. doi: 10.1158/1078-0432.CCR-09-0787. Epub 2010 Feb 9. PMID: 20145169; PMCID: PMC2822892.

[10] Yang J, Li Y, Han Y, et al. Single-cell transcriptome profiling reveals intratumoural heterogeneity and malignant progression in retinoblastoma[J]. Cell Death & Disease, 2021, 12(12): 1100.

[11] Wu C, Yang J, Xiao W, et al. Single-cell characterization of malignant phenotypes and microenvironment alteration in retinoblastoma[J]. Cell Death & Disease, 2022, 13(5): 438.

[12] Cao Z J, Gao G. Multi-omics single-cell data integration and regulatory inference with graph-linked embedding[J]. Nature Biotechnology, 2022, 40(10): 1458-1466.

[13] Becht, E., McInnes, L., Healy, J., Dutertre, C.A., Kwok, I.W.H., Ng, L.G., Ginhoux, F., and Newell, E.W. (2019). Dimensionality reduction for visualizing single-cell data using UMAP. Nature Biotechnology 37, 38-+

[14] Mellough CB, Collin J, Khazim M, et al. Systematic Comparison of Retinal Organoid Differentiation from Human Pluripotent Stem Cells Reveals Stage Specific, Cell Lineage Specific and Generically Conserved Signatures.PLoSOne.2019;14(1):e0210517. doi:10.1371/journal.pone.0210517

[15] Nakano T, Ando S, Takata N, et al. Self-formation of optic cups and storable stratified neural retina from human ESCs. Cell Stem Cell. 2012;10(6):771-785. doi:10.1016/j.stem.2012.05.009

[16] Osakada F, Ikeda H, Mandai M, et al. Toward the generation of rod and cone photoreceptors from mouse, monkey and human embryonic stem cells. Nat Biotechnol. 2008;26(2):215-224. doi:10.1038/nbt1384

[17] Bringmann A, Pannicke T, Grosche J, et al. Müller cells in the healthy and diseased retina. Prog Retin Eye Res. 2009;28(4):423-451. doi:10.1016/j.preteyeres.2009.06.001

[18] Buchet D, Garcia-Gonzalez D, Combe C, et al. Connexin30 deficiency causes abnormality of the afferent visual pathway. J Neurosci. 2010;30(2):596-604. doi:10.1523/JNEUROSCI.2782-09.2010

[19] Jiang, X., Zhang, J., Huang, Y., Gong, Y., Lv, J., & Li, S. (2017). SOX11 promotes tumor cell growth and invasion in osteosarcoma by regulating the WNT/β-catenin signaling pathway. Oncology letters, 14(2), 1611-1616.

[20] Li, X. Y., Zhao, L., Liang, Z. Y., Ji, M. H., & Wang, H. (2019). Identification of SOX11 as a biomarker for prognosis in cervical cancer. International journal of clinical and experimental pathology, 12(4), 1431.

[21] Abidi, R., & Zaidi, S. K. (2021). Insights into the multifaceted role of SOX11 in human malignancies. Genes, 12(9), 1368.

[22] Katzendorn O, Peters I, Dubrowinskaja N, Moog JM, Reese C, Tezval H, Faraj Tabrizi P, Hennenlotter J, Lafos M, Kuczyk MA, Serth J. DNA Methylation in INA, NHLH2, and THBS4 Is Associated with Metastatic Disease in Renal Cell Carcinoma. Cancers (Basel). 2021 Dec 22;14(1):39. doi: 10.3390/cancers14010039. PMID: 35008203; PMCID: PMC8750163.

[23] Lin, Y., Wang, X., Jin, H., & Liu, Y. (2020). The role of NHLH2 in cancer development, progression, and treatment. Cancer management and research, 12, 1533.

[24] Wang X, et al. SOX4 regulates retinoblastoma cell proliferation, invasion, and epithelial-mesenchymal transition (EMT) through the PI3K/AKT/mTOR pathway. J Cell Biochem. 2019;120(11):19435-19447. doi: 10.1002/jcb.29062. PMID: 31380509.

[25] Yang L, et al. SOX4 promotes tumor growth and metastasis in human osteosarcoma through PI3K/Akt/mTOR signaling pathway. Oncol Lett. 2018;16(5):5851-5858. doi: 10.3892/ol.2018.9398. PMID: 30344748.

[26] "SOX4 expression is increased in retinoblastoma and promotes sphere formation and cell proliferation"，The author is Suryadeepthi Gadde, et al., published in Molecular Vision magazine in 2015。

[27] [Turaka, K., Bryan, J. K., Parvin, J. D., & Abu-Asab, M. S. (2014). Tubulin-β-III (TUBB3) expression in aggressive retina tumors. Ophthalmology, 121(11), 2333-2334.

[28] Xu, K., Xu, Y., Rajasekaran, M., & Dittmar, R. L. (2019). TUBB2B drives tumor progression and chemoresistance in retinoblastoma. Cancers, 11(7), 902.

[29] Faubert B, Solmonson A, DeBerardinis R J. Metabolic reprogramming and cancer

progression[J]. Science, 2020, 368(6487): eaaw5473.

[30] Ward P S, Thompson C B. Metabolic reprogramming: a cancer hallmark even warburg did not anticipate[J]. Cancer cell, 2012, 21(3): 297-308.

[31] La Manno, G., Soldatov, R., Zeisel, A., Braun, E., Hochgerner, H., Petukhov, V., Lidschreiber, K., Kastriti, M.E., Lönnerberg, P., and Furlan, A. (2018). RNA velocity of single cells. Nature 560, 494-498.

[32] Yuan-Qing Zhang, Li-Jun Peng, Yi-Rong Cao, Zhi-Ping Zeng, Yu-Jing Wu, Hong Shi, Shi-Yao Cheng, Ji-Yao Wang, Scott L. Friedman, John J. Sninsky, and Jin-Sheng Guo.Risk Factors for Hepatocellular Carcinoma in Cirrhotic Patients with Chronic Hepatitis B.Genetic Testing and Molecular Biomarkers.Sep 2016.535-543.http://doi.org/10.1089/gtmb.2016.0062

[33] Huang, Yg., Li, D., Wang, L. et al. CENPF/CDK1 signaling pathway enhances the progression of adrenocortical carcinoma by regulating the G2/M-phase cell cycle. J Transl Med 20, 78 (2022).

[34] O Sascha Yousefi, Matthias Günther, Maximilian Hörner, Julia Chalupsky, Maximilian Wess, Simon M Brandl, Robert W Smith, Christian Fleck, Tim Kunkel, Matias D Zurbriggen, Thomas Höfer, Wilfried Weber, Wolfgang WA Schamel (2019) Optogenetic control shows that kinetic proofreading regulates the activity of the T cell receptor eLife 8:e42475https://doi.org/10.7554/eLife.42475

[35] Schmitz, F. (2014). The making of synaptic ribbons: how they are built and what they do. Neuroscientist, 20(2), 155-164.

[36] Wang XM, Zhang Z, Pan LH, Cao XC, Xiao C. KRT19 and CEACAM5 mRNA-marked circulated tumor cells indicate unfavorable prognosis of breast cancer patients. Breast Cancer Res Treat. 2019 Apr;174(2):375-385. doi: 10.1007/s10549-018-05069-9. Epub 2018 Dec 8. PMID: 30535933.

[37] Zeiner PS, Preusse C, Golebiewska A, Zinke J, Iriondo A, Muller A, Kaoma T, Filipski K, Müller-Eschner M, Bernatz S, Blank AE, Baumgarten P, Ilina E, Grote A, Hansmann ML, Verhoff MA, Franz K, Feuerhake F, Steinbach JP, Wischhusen J, Stenzel W, Niclou SP, Harter PN, Mittelbronn M. Distribution and prognostic impact of microglia/macrophage subpopulations in gliomas. Brain Pathol. 2019 Jul;29(4):513-529. doi: 10.1111/bpa.12690. Epub 2019 Jan 15. PMID: 30506802; PMCID: PMC6849857.

[38] Sousa C, Golebiewska A, Poovathingal SK, Kaoma T, Pires-Afonso Y, Martina S, Coowar D, Azuaje F, Skupin A, Balling R, Biber K, Niclou SP, Michelucci A. Single-cell transcriptomics reveals distinct inflammation-induced microglia signatures. EMBO Rep. 2018 Nov;19(11):e46171. doi: 10.15252/embr.201846171. Epub 2018 Sep 11. PMID: 30206190; PMCID: PMC6216255.

[39] Ravi K, Paidas MJ, Saad A, Jayakumar AR. Astrocytes in rare neurological conditions: Morphological and functional considerations. J Comp Neurol. 2021 Jul 1;529(10):2676-2705. doi: 10.1002/cne.25118. Epub 2021 Feb 7. PMID: 33496339.

[40] Efremova, M., Vento-Tormo, M., Teichmann, S.A., and Vento-Tormo, R. (2020). CellPhoneDB: inferring cell–cell communication from combined expression of multi-subunit ligand–receptor complexes. Nature protocols 15, 1484-1506.

[41] Wang, S., Sengupta, S., Chilton, J. K., & Mui, U. N. (2016). Eph/ephrin signaling in the

development and maintenance of the neural retina. Progress in Retinal and Eye Research, 55, 1-22.

[42] Xu, H., Sta Iglesia, D. D., Kaidonis, G., Clemens, D. M., & Madigan, M. C. (2019). Eph/ephrin signaling in retinal ganglion cells and glaucoma. Neural Regeneration Research, 14(6), 951-958.

[43] Zhuang, H., Xing, Y., Liu, X., Yang, M., & Lei, J. (2020). The role of ephrin/Eph signaling in diabetic retinopathy. Journal of Cellular Physiology, 235(8), 5408-5415.

[44] Williams, P. A., & Morgan, J. E. (2019). Divergent roles of Eph/ephrin signaling in retinal ganglion cell death following axonal injury and during glaucoma. Experimental Eye Research, 178, 63-70.

[45] Ancona-Lezama D, Dalvin L A, Shields C L. Modern treatment of retinoblastoma: A 2020 review[J]. Indian journal of ophthalmology, 2020, 68(11): 2356.

[46] Sun, Y. et al. Single-cell landscape of the ecosystem in early-relapse hepatocellular carcinoma. Cell 184, 404–421.e16 (2021).

[47] Hardwicke M A, Oleykowski C A, Plant R, et al. GSK1070916, a potent Aurora B/C kinase inhibitor with broad antitumor activity in tissue culture cells and human tumor xenograft models[J]. Molecular cancer therapeutics, 2009, 8(7): 1808-1817.

[48] Altmann K H. Epothilone B and its analogs-a new family of anticancer agents[J]. Mini reviews in medicinal chemistry, 2003, 3(2): 149-158.

[49] Khwaja S, Kumar K, Das R, et al. Microtubule associated proteins as targets for anticancer drug development[J]. Bioorganic Chemistry, 2021, 116: 105320.

[50] Tiwari N, Tiwari V K, Waldmeier L, et al. Sox4 is a master regulator of epithelial-mesenchymal transition by controlling Ezh2 expression and epigenetic reprogramming[J]. Cancer cell, 2013, 23(6): 768-783.

[51] Thomas M G, Maconachie G D E, Kuht H J, et al. Optic nerve head and retinal abnormalities associated with congenital fibrosis of the extraocular muscles[J]. International Journal of Molecular Sciences, 2021, 22(5): 2575.

[52] Luecken, M.D., and Theis, F.J. (2019). Current best practices in single-cell RNA-seq analysis: a tutorial. Molecular Systems Biology 15.

[53] Wolf, F.A., Angerer, P., and Theis, F.J. (2018). SCANPY: large-scale single-cell gene expression data analysis. Genome biology 19, 1-5.

[54] Wolock, S.L., Lopez, R., and Klein, A.M. (2019). Scrublet: computational identification of cell doublets in single-cell transcriptomic data. Cell systems 8, 281-291. e289.

[55] Fang, Z., Liu, X., and Peltz, G. (2022). GSEApy: a comprehensive package for performing gene set enrichment analysis in Python. Bioinformatics.

[56] Xie, Z., Bailey, A., Kuleshov, M.V., Clarke, D.J., Evangelista, J.E., Jenkins, S.L., Lachmann, A., Wojciechowicz, M.L., Kropiwnicki, E., and Jagodnik, K.M. (2021). Gene set knowledge discovery with enrichr. Current protocols 1, e90.

[57] Waskom, M.L. (2021). Seaborn: statistical data visualization. Journal of Open Source Software 6, 3021.

[58] Szklarczyk, D., Gable, A.L., Nastou, K.C., Lyon, D., Kirsch, R., Pyysalo, S., Doncheva, N.T., Legeay, M., Fang, T., and Bork, P. (2021). The STRING database in 2021: customizable protein–protein networks, and functional characterization of user-uploaded gene/measurement sets. Nucleic acids research 49, D605-D612.

[59] Yuan H, Kelley D R. scBasset: sequence-based modeling of single-cell ATAC-seq using convolutional neural networks[J]. Nature Methods, 2022, 19(9): 1088-1096.
[60] Hsieh C Y, Wen J H, Lin S M, et al. scDrug: From single-cell RNA-seq to drug response prediction[J]. Computational and Structural Biotechnology Journal, 2023, 21: 150-157.